OPEN

NPG Asia Materials (2013) 5, e60; doi:10.1038/am.2013.38

www.nature.com/am

ORIGINAL ARTICLE

Enhancing the short-circuit current and power conversion efficiency of polymer solar cells with graphene quantum dots derived from double-walled carbon nanotubes

Fushan Li, Lijie Kou, Wei Chen, Chaoxing Wu and Tailiang Guo

Derived from double-walled carbon nanotubes, graphene quantum dots (GQDs) with a uniform size distribution were prepared through solution chemistry. The GQDs in chlorobenzene exhibited bright blue emission upon UV excitation. The introduction of the GQDs into a bulk heterojunction polymer solar cell based on poly(3-hexylthiophene):(6,6)-phenyl-C61 butyric acid methyl ester (P3HT:PCBM) resulted in a significant enhancement of the power conversion efficiency (PCE). The efficiency was further improved by adjusting the PCBM content in the active layer, reaching a maximum PCE of 5.24%. This ternary system based on blended P3HT:PCBM:GQDs represents a new method to enhance the efficiency of polymer solar cells.
NPG Asia Materials (2013) **5,** e60; doi:10.1038/am.2013.38; published online 23 August 2013

Keywords: graphene quantum dots; polymer solar cells; power conversion efficiency; short-circuit current

INTRODUCTION

Polymer solar cells (PSCs) have received broad attention and are regarded as the most promising technology for the plastic photovoltaic industry because they provide a general route to achieve large-area, low-cost, flexible photovoltaic devices.[1–5] In this type of device, a blend of an electron-donating material (p-type conjugated polymers) and an electron-accepting material (n-type fullerene derivatives) is used to form a bulk heterojunction active layer. One of the most representative bulk heterojunction PSCs is the device based on a blend of poly(3-hexylthiophene) (P3HT) as an electron donor and the fullerene derivative (6,6)-phenyl-C61 butyric acid methyl ester (PCBM) as an electron acceptor.[6–8] The donor and acceptor are naturally nanostructured due to the phase segregation of the polymer and the fullerene derivative. However, the power conversion efficiency (PCE) of the optimized devices is still not high enough for practical applications.[9] Increasing this efficiency even further requires the introduction of new materials with improved photovoltaic properties and a detailed analysis of the device performance based on these materials.

Quantum dots (for example, CdSe and PbTe) have been widely used as electron acceptor materials in photovoltaics due to their size-dependent optical response, efficient multiple carrier generation and low cost.[10–14] However, their toxicity and hazardous nature are serious drawbacks for large-scale device applications. It has been demonstrated that graphene quantum dots (GQDs) blended with P3HT resulted in a significant improvement in PSC characteristics compared to graphene sheets blended with conjugated polymers.[15] However, the obtained PCE for the GQDs-based PSC was rather low (~1%). Here, we show that for PSC applications, light-emitting GQDs derived from double-walled carbon nanotubes (DCNTs) can be used as an excellent supplement to P3HT:PCBM, rather than a replacement. This ternary system based on P3HT:PCBM:GQDs blends can serve as the active layer for a PSC with a significantly enhanced PCE.

EXPERIMENTAL PROCEDURES

Synthesis of the GQDs

As shown in Figure 1, the GQDs were derived from commercially available DCNTs. The DCNTs were added to a mixture of concentrated H_2SO_4 (10 ml) and HNO_3 (5 ml). The solution was kept at room temperature for 4 h and stirred at 100 °C for 24 h. After cooling to room temperature, the suspension was ultrasonicated for 4 h. Subsequently, the mixture was diluted with deionized water (60 ml), and the pH was adjusted to 8 with NaOH solution. After dialyzing in a dialysis bag (retained molecular weight: 2000 Da) for 4 days, the product solution was centrifuged for 1.5 h in an ultrafiltration centrifugal tube (retained molecular weight: 3000 Da, purchased from Shanghai Jinxin Biotechnology Corporation, Shanghai, China). The solution was mixed with chlorobenzene in a 1:1 ratio, followed by violent shaking and stirring. After standing for 1 h, the bottom solution was extracted, which included the GQDs with a uniform size distribution.

Characterization of the GQDs

High-resolution transmission electron microscopy measurements were carried out to investigate the microstructural properties of the GQDs. The specimen

Institute of Optoelectronic Technology, Fuzhou University, Fuzhou, People's Republic of China
Correspondence: Professor F Li or Professor T Guo, Institute of Optoelectronic Technology, Fuzhou University, 523 Gongye Road, Fuzhou 350002, People's Republic of China.
E-mails: fushanli@hotmail.com or gtl_fzu@hotmail.com
Received 14 March 2013; revised 12 June 2013; accepted 18 June 2013

was prepared by drop casting the sample dispersion onto a carbon-coated copper grid, followed by drying at room temperature. Photoluminescence (PL) spectra of the GQDs were obtained with a fluorescence spectrophotometer (Hitachi, Tokyo, Japan, F-4600). Atomic force microscopy measurements were acquired with a Nanoscope IIIa in tapping mode. The UV–vis spectra were obtained with a Shimadzu UV3600 spectrophotometer (Shimadzu, Kyoto, Japan).

Fabrication and characterization of the GQDs-based PSCs

For the fabrication of the GQDs-based PSCs, P3HT (10 mg ml^{-1}) solutions with PCBM contents of 0.5, 0.6, 0.8, 1, 1.25, 1.67 and 2 (weight ratio to P3HT) were prepared in chlorobenzene. The GQDs were added to the solution at a concentration of 0.05 mg ml^{-1}. The solution was then spin-cast on indium tin oxide (ITO) glass substrates and coated with poly(ethylenedioxythiophene):-poly(styrene sulfonic acid) (PEDOT:PSS) conductive polymer, which served as the bottom electrode. LiF and Al were deposited by thermal evaporation as the top contact to form a PSC device with the structure ITO/PEDOT:PSS/P3HT:PCBM:GQDs/LiF/Al. The active area of the PSCs was 0.1 cm^2. For comparison, a PSC without GQDs was also fabricated. The characterization of the as-fabricated PSCs was carried out with a solar simulator (Abet Sun 2000; Abet Technologies, Milford, CT, USA) under 100 mW AM 1.5G illumination. The current density–voltage (*J*–*V*) characteristics were collected with a Keithley 4200 semiconductor characterization system (Keithley, Cleveland, OH, USA).

RESULTS AND DISCUSSION

The high-resolution transmission electron microscopy images of the DCNTs-derived GQDs are shown in Figure 2. The diameters of the GQDs are mainly distributed in the range of 3–5 nm, with an average diameter of 4 nm (Figure 2a). Figure 2b shows a representative image of an individual GQD that is highly crystalline, with a lattice parameter of 0.322 nm, which is in good agreement with a previous report.[16] The atomic force microscopy analysis shown in Figure 2c is also in agreement with the TEM results. The GQDs (deposited on a Si substrate) are estimated to have an average height of ~2 nm, which is associated with a bilayer graphene structure.

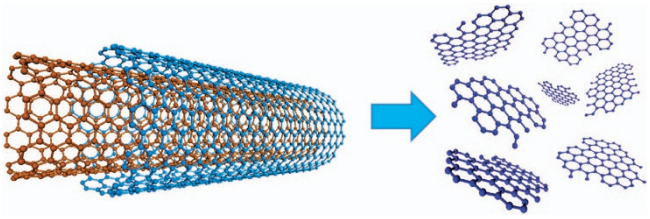

Figure 1 Schematic showing the preparation of the GQDs from DCNTs.

Under 365 nm UV illumination, the GQDs exhibited bright blue emission, as shown in the inset of Figure 3. To further explore the optical properties of the GQDs, the PL spectra were recorded and are shown in Figure 3. Similar to previous reports, the GQDs exhibited an excitation-dependent PL behavior.[17] Changing the excitation wavelength from 310 nm to 510 nm in 20-nm steps gradually shifted the PL peak to longer wavelengths. This excitation-dependent PL behavior has been extensively reported in fluorescent carbon-based nanomaterials and may be related to the inhomogeneities of the orbital energy distribution of the defect states.[18]

Figure 4 shows the UV–vis absorption spectra of the P3HT:PCBM blended (weight ratio 1:1) films with and without the GQDs. A film thickness of 100 nm was used to normalize the absorption intensity of the blend. As shown in Figure 4, both blends exhibit vibronic absorption shoulders at ~335, 510, 552 and 600 nm in the visible region, which can be ascribed to the absorption of PCBM and P3HT. The peak at 335 nm is the absorption of PCBM, and the peak at 510 nm is the absorption of the P3HT main chain. The other two peaks at longer wavelengths are due to the interchain interactions in the ordered P3HT crystalline regions in the blend.[19] The introduction of the GQDs results in an enhancement of the absorption peaks and also leads to a slight redshift of the P3HT absorption peaks. This finding indicates that the interchain interactions are improved by the addition of the GQDs to the blend.

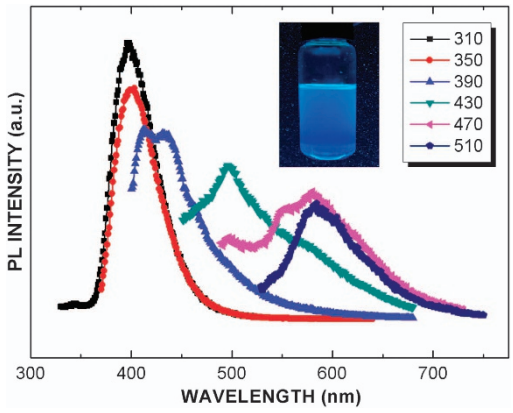

Figure 3 PL spectra of the as-prepared GQDs with various excitation wavelengths. Inset: photograph of the GQDs in chlorobenzene taken under 365 nm UV light.

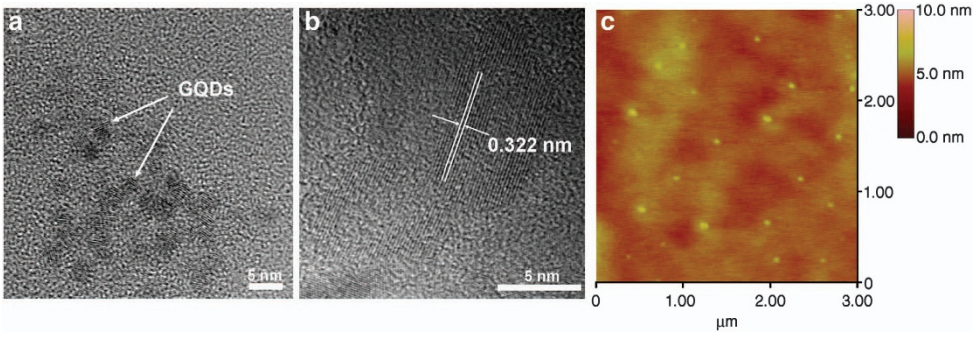

Figure 2 (**a**) TEM image of the as-prepared GQDs. (**b**) High-resolution TEM image showing the crystal structure of an individual GQD. (**c**) Atomic force microscopy image of the GQDs deposited on a Si substrate.

Figure 5a shows the *J–V* characteristics of the PSCs with and without GQDs, and Figure 5b illustrates the *J–V* curves for the GQDs-based PSCs with various PCBM contents. The obtained PCE, open-circuit voltage (V_{oc}), short-circuit current density (J_{sc}) and fill factor (FF) of the as-fabricated PSCs are summarized in Table 1. The introduction of the GQDs has an obvious effect on the photovoltaic performances of the P3HT:PCBM-based PSCs. The PSC without GQDs delivers a PCE of 2.61% with a V_{oc} of 0.59 V, a J_{sc} of 14.27 mA cm^{-2}, and a FF of 0.31. After adding the GQDs into the active layer, the V_{oc}, J_{sc}, FF and PCE of the device are 0.57 V, 24.6 mA cm^{-2}, 0.31 and 4.35%, respectively. In comparison with the conventional P3HT:PCBM-based PSCs, the PCE of the device based on the P3HT:PCBM:GQDs ternary blends is significantly improved.

Considering the structural similarity of GQDs and PCBM, the PCBM content in the active layer is varied to optimize the device performance. As shown in Table 1, the J_{sc} of the PSCs is strongly dependent on the PCBM content in the ternary blend. Consequently, the PCE of the P3HT:PCBM:GQDs-based PSCs can be tailored by varying the weight ratio of PCBM to P3HT, as shown in Figure 6. As the PCBM:P3HT weight ratio increases from 0.5–0.6, the PCE of the device increases dramatically from 2.48–5.24%, which is the highest efficiency achieved in this work. However, higher PCBM content does not translate to better device performance when the PCBM:P3HT weight ratio exceeds 0.6. The PCE of the PSC decreases gradually

Table 1 Performance details of the PSCs based on the P3HT:PCBM:GQDs ternary blends under simulated AM 1.5G 100 mW illumination

Sample no.	*P3HT:PCBM (weight ratio)*	*Short-circuit current density (mA cm^{-2})*	*Open-circuit voltage (V)*	*Fill factor*	*Power conversion efficiency (%)*
1	1:1 (without GQD)	14.27	0.59	0.31	2.61 ± 0.3
2	2:1	15.54	0.57	0.28	2.48 ± 0.1
3	1:0.6	26.46	0.60	0.33	5.24 ± 0.4
4	1:0.8	23.5	0.60	0.31	4.37 ± 0.1
5	1:1	24.6	0.57	031	4.35 ± 0.1
6	0.8:1	23.96	0.57	0.28	3.85 ± 0.3
7	0.6:1	22.2	0.57	0.30	3.83 ± 0.2
8	1:2	11.8	0.56	0.31	2.05 ± 0.4

Abbreviations: GQD, graphene quantum dots; P3HT:PCBM, poly (3-hexylthiophene):(6,6)-phenyl-C61 butyric acid methyl ester.

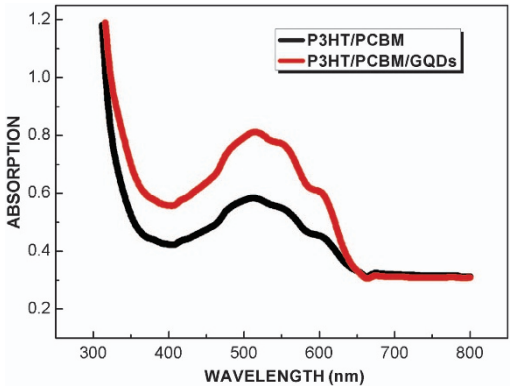

Figure 4 UV–vis absorption spectra of the P3HT:PCBM (weight ratio 1:1) blended films with and without GQDs.

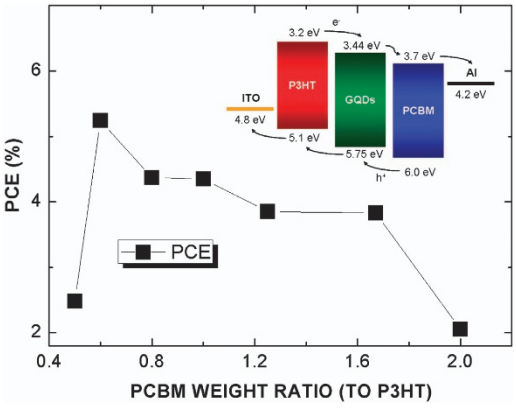

Figure 6 PCE of the PSCs with varying PCBM:P3HT weight ratios. Inset: band diagram showing the working process of the PSCs with GQDs. The highest occupied molecular orbital and lowest unoccupied molecular orbital values of the P3HT, PCBM, and GQDs are taken from the literature (Gupta *et al.*[15], Wang *et al.*[25] and Gupta *et al.*[15] respectively).

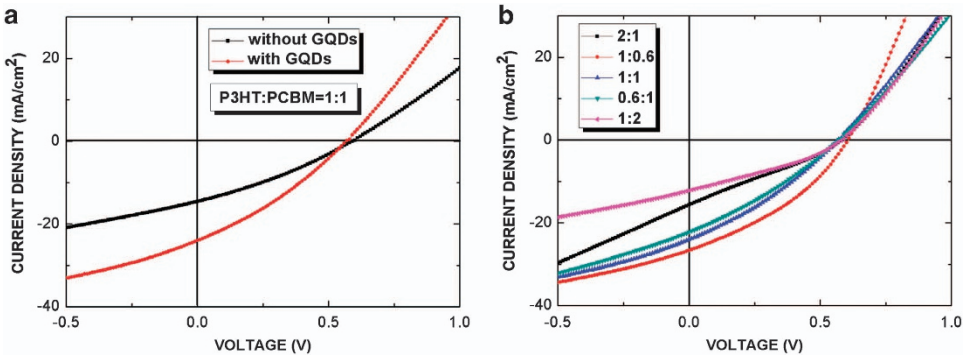

Figure 5 (**a**) J_{sc}–*V* characteristics of the PSCs based on P3HT:PCBM (weight ratio 1:1) blended films with and without GQDs. (**b**) J_{sc}–*V* curves of the PSCs based on the P3HT:PCBM:GQDs ternary blends with various PCBM contents.

starting at that point, and when the PCBM:P3HT weight ratio reaches 2, the PCE of the device is only 2.05%.

The ratio of donor and acceptor materials in formulating an efficient bulk heterojunction layer is an important parameter that controls the morphological, charge transport and exciton dissociation properties of the constituents.[20] When the PCBM content is low (0.5 weight ratio to P3HT), the matrix is fairly homogeneous.[21] The J_{sc} and PCE are significantly enhanced with the increase of the PCBM ratio to 0.6 due to the emergence of a phase separation, which result in enhanced charge carrier transport and a reduction in bimolecular charge recombination.[22] However, with a further increase of the PCBM ratio (>0.6), the decreasing optical density of the film due to the low absorption cross section of PCBM compared to P3HT eventually leads to a drop in the J_{sc} and PCE.

It is important to note that for the ternary blend-based PSCs, the best device performance is obtained at a PCBM ratio of 0.6, which is lower than the typical values (1 and 0.8) reported previously.[23,24] Additionally, the PCE of the ternary blend-based PSC is much higher than that of the conventional device with the same PCBM ratio, which must be attributed to the presence of the GQDs in the active layer. The band diagram illustrating the working process of the PSCs with GQDs is shown in the inset of Figure 6. It is proposed that the unique band structure of the GQDs narrows the energy barrier between the highest occupied molecular orbital and the lowest unoccupied molecular orbital levels between P3HT and PCBM, which favors the transport of the photogenerated holes and electrons, as shown in the inset of Figure 6. In addition, as mentioned above, the existence of the GQDs also contributes to the improvement of the absorption of the P3HT:PCBM blend. As a result, the exciting enhancement of the J_{sc} and PCE of the P3HT:PCBM blend-based PSC can be achieved by introducing GQDs in the active layer.

CONCLUSIONS

In conclusion, GQDs are synthesized from DCNTs with a uniform size distribution through solution chemistry, and the GQDs in chlorobenzene exhibit bright blue emission upon UV excitation. The PCE of the PSC based on the P3HT:PCBM:GQDs ternary blends is significantly improved compared to that of the conventional P3HT:PCBM-based device. The device performance can be further improved by varying the PCBM concentration in the ternary active layer, resulting in a maximum PCE of 5.24%. This improvement is attributed to the enhanced absorption of the blended film and the unique band structure of the GQDs. The ternary system based on the P3HT:PCBM:GQDs blends represents a new method to meet the high demand for polymer solar cells with enhanced efficiency. In addition, this work expands the application of GQDs to PSC devices.

ACKNOWLEDGEMENTS

This work was supported by the Specialized Research Fund for the Doctoral Program of Higher Education of China (20103514120009), the Scientific Research Project for Universities funded by the Fujian Education Department (JK2010005) and the National High Technology Research and Development Program of China (863 Program, 2012AA030303).

1 Gunes, S., Neugebauer, H. & Sariciftci, N. S. Conjugated polymer-based organic solar cells. *Chem. Rev.* **107,** 1324–1338 (2007).
2 Roncali, J. Molecular bulk heterojunctions: an emerging approach to organic solar cells. *Acc. Chem. Res.* **42,** 1719–1730 (2009).
3 Meissner, D. & Wohrle, D. Organic solar cells. *Adv. Mater.* **3,** 129–138 (1991).
4 Huynh, W. U., Dittmer, J. J. & Alivisatos, P. A. Hybrid nanorod-polymer solar cells. *Science* **295,** 2425–2427 (2002).
5 Padinger, F., Rittberger, R. S. & Sariciftci, N. S. Effects of postproduction treatment on plastic solar cells. *Adv. Funct. Mater.* **13,** 85–88 (2003).
6 Hwang, I., Moses, D. & Heeger, A. J. Photoinduced carrier generation in P3HT/PCBM bulk heterojunction materials. *J. Phys. Chem. C* **112,** 4350–4354 (2008).
7 Vanlaeke, P., Swinnen, A., Haeldermans, I., Vanhoyland, G., Aernouts, T., Cheyns, D., Deibel, C., Dhaen, J., Heremans, P., Poortmans, J. & Manca, J. V. P3HT/PCBM bulk heterojunction solar cells: relation between morphology and electro-optical characteristics. *Sol. Energy Mater. Sol. Cells* **90,** 2150–2158 (2006).
8 Hauch, J. A., Schilinsky, P., Choulis, S. A., Childers, R., Biele, M. & Brabec, C. J. Flexible organic P3HT: PCBM bulk-heterojunction modules with more than 1 year outdoor lifetime. *Sol. Energy Mater. Sol. Cells* **92,** 727–731 (2008).
9 Chen, D., Liu, F., Wang, C., Nakahara, A. & Russell, T. P. Bulk heterojunction photovoltaic active layers via bilayer interdiffusion. *Nano Lett.* **11,** 2071–2078 (2011).
10 Koleilat, G. I., Levina, L., Shukla, H., Myrskog, S. H., Hinds, S., Pattantyus-Abraham, A. G. & Sargent, E. H. Efficient, stable infrared photovoltaics based on solution-cast colloidal quantum dots. *ACS Nano* **2008,** 833–840 (2008).
11 Vavilov, M. G., Ambegaokar, V. & Aleiner, I. L. Charge pumping and photovoltaic effect in open quantum dots. *Phys. Rev. B* **63,** 195313 (2001).
12 Barkhouse, D. A. R., Pattantyus-Abraham, A. G., Levina, L. & Sargent, E. H. Thiols passive recombination centers in colloidal quantum dots leading to enhanced photovoltaic device efficiency. *ACS Nano* **2,** 2356–2362 (2008).
13 Mcdonald, S. A., Konstantatos, G., Zhang, S., Cyr, P. W., Klem, E. J. D., Levina, L. & Sargent, E. H. Solution-processed PbS quantum dot infrared photodetectors and photovoltaics. *Nat. Mater.* **4,** 138–142 (2005).
14 Noone, K. M., Strein, E., Anderson, N. C., Wu, P., Jenekhe, S. A. & Ginger, D. S. Broadband absorbing bulk heterojunction photovoltaics using low-bandgap solution processed quantum dots. *Nano Lett.* **10,** 2635–2639 (2010).
15 Gupta, V., Chaudhary, N., Srivastava, R., Sharma, G. D., Bhardwaj, R. & Chand, S. Luminescent graphene quantum dots for organic photovoltaic devices. *J. Am. Chem. Soc.* **133,** 9960–9963 (2011).
16 Peng, J., Gao, W., Gupta, B. K., Liu, Z., Romero-Aburto, R., Ge, L., Song, L., Alemany, L. B., Zhan, X., Gao, G., Vithayathil, S. A., Kaipparettu, B. A., Marti, A. A., Hayashi, T., Zhu, J. & Ajayan, P. M. Graphene quantum dots derived from carbon fiber. *Nano Lett.* **12,** 844–849 (2012).
17 Pan, D. Y., Zhang, J. C., Li, Z. & Wu, M. H. Hydrothermal route for cutting graphene sheets into blue-luminescent graphene quantum dots. *Adv. Mater.* **22,** 734–738 (2010).
18 Riggs, J. E., Guo, Z. L., Carroll, D. & Sun, Y. P. Strong luminescence of solubilized carbon nanotubes. *J. Am. Chem. Soc.* **122,** 5879–5880 (2000).
19 Li, G., Shrotriya, V., Huang, J., Yao, Y., Moriarty, T., Emery, K. & Yang, Y. High-efficiency solution processable polymer photovoltaic cells by self-organization of polymer blends. *Nat. Mater.* **4,** 864–868 (2005).
20 Zhao, G., He, Y. & Li, Y. 6.5% efficiency of polymer solar cells based on poly(3-hexylthiophene) and indene-C60 bisadduct by device optimization. *Adv. Mater.* **22,** 4355–4358 (2010).
21 Kumar, P. & Chand, S. Recent progress and future aspects of organic solar cells. *Prog. Photovolt: Res. Appl.* **20,** 377–415 (2012).
22 Duren, J. K. J., Yang, X., Loos, J., Bulle-lieuwma, C. W. T., Sieval, A. B., Hummelen, J. C. & Janssen, R. A. J. Relating the morphology of poly(p-phenylene vinylene)/methanofullerene blends to solar cell performance. *Adv. Funct. Mater.* **14,** 425–434 (2004).
23 Bettignes, R. D., Leroy, J., Firon, M. & Sentein, C. Accelerated lifetime measurements of P3HT:PCBM solar cells. *Synth. Met.* **156,** 510–513 (2006).
24 Kim, J. Y., Kim, S. H., Lee, H., Lee, K., Ma, W., Gong, X. & Heeger, A. J. New architecture for high-efficiency polymer photovoltaic cells using solution-based titanium oxide as an optical spacer. *Adv. Mater.* **18,** 572–576 (2006).
25 Wang, D. H., Lee, H. K., Choi, D., Park, J. H. & Park, O. O. Solution-processable polymer solar cells from a poly(3-hexylthiophene)/[6,6]-phenyl C61-butyric acidmethyl ester concentration graded bilayers. *Appl. Phys. Lett.* **95,** 043505 (2009).